QTAIM charge–charge flux–dipole flux models for the fundamental infrared intensities of BF_3 and BCl_3

ARTICLE *in* SPECTROCHIMICA ACTA PART A MOLECULAR AND BIOMOLECULAR SPECTROSCOPY · JULY 2013

Impact Factor: 2.35 · DOI: 10.1016/j.saa.2013.07.005 · Source: PubMed

5 AUTHORS, INCLUDING:

Wagner E Richter
University of Campinas
12 PUBLICATIONS **20** CITATIONS
SEE PROFILE

Arnaldo F. Silva
University of Campinas
11 PUBLICATIONS **20** CITATIONS
SEE PROFILE

Pedro A. M. Vazquez
University of Campinas
33 PUBLICATIONS **131** CITATIONS
SEE PROFILE

Roy E. Bruns
University of Campinas
255 PUBLICATIONS **3,220** CITATIONS
SEE PROFILE

Spectrochimica Acta Part A: Molecular and Biomolecular Spectroscopy 116 (2013) 136–142

Contents lists available at ScienceDirect

Spectrochimica Acta Part A: Molecular and Biomolecular Spectroscopy

journal homepage: www.elsevier.com/locate/saa

QTAIM charge–charge flux–dipole flux models for the fundamental infrared intensities of BF_3 and BCl_3

Wagner E. Richter, Arnaldo F. Silva, Andrew C.L. Pitoli, Pedro A.M. Vazquez, Roy E. Bruns *

Instituto de Química, Universidade Estadual de Campinas, 13083–970 Campinas, SP, Brazil

HIGHLIGHTS

- Charge–charge flux dipole flux model for infrared intensities of BF_3 and BCl_3.
- Spectroscopic evidence of high ionicity of BF_3 bonds.
- BF and BCl bends described by equilibrium charge movement and dipole fluxes.
- BF and BCl stretching vibrations described by equilibrium charge movement.
- BF, BCl, CF and CCl stretching vibrations have similar electronic changes.

GRAPHICAL ABSTRACT

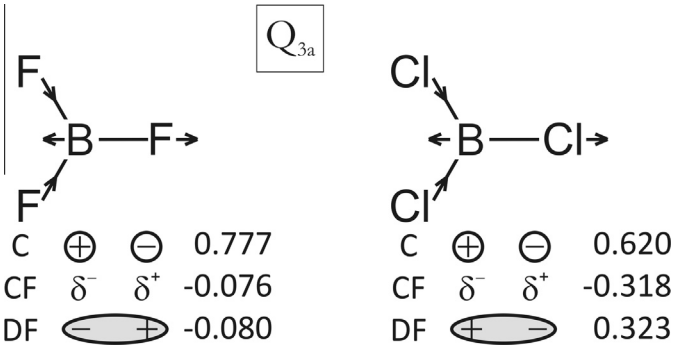

ARTICLE INFO

Article history:
Received 16 April 2013
Received in revised form 27 June 2013
Accepted 1 July 2013
Available online 11 July 2013

Keywords:
Atoms in molecules
QTAIM/CCFDF
Infrared intensities
BF_3
Bond character

ABSTRACT

Quantum Theory of Atoms in Molecules Charge–Charge Flux–Dipole Flux (QTAIM/CCFDF) models have been determined for the BF_3 and BCl_3 molecules. Model parameters were obtained from MP2/6–31G(2d,2p) wave functions owing to their accurate estimations of the BF_3 intensities and were found to be insensitive to changes in basis sets with polarization functions and to the level of electron correlation treatment, MP2, QCISD and DFT. The BF_3 stretching intensity has a very dominant equilibrium charge contribution with small charge and dipole fluxes occurring in the opposite direction to the charge movement. Large equilibrium charge and small dynamic contributions are also characteristic of stretching vibrations in the ionic diatomic molecules, NaF, NaCl, LiF and LiCl. Furthermore the Laplacians of the electron density at the bond critical points of BF_3 and these diatomics are all positive indicating electron depletion in their bonding regions relative to large electronic densities concentrated around their nuclei that is characteristic of ionic bonds. The MP2/6–31G(2d,2p) BCl_3 stretching intensity can be accurately estimated by equilibrium charge movement since the charge and dipole fluxes almost exactly cancel one another. Both in-plane and out-of-plane BF_3 and BCl_3 bending deformations are described by equilibrium charge movements that are partially canceled by opposing dipole fluxes that measure the effect on the dipole moment change from electron densities polarized in the opposite direction. Charge fluxes are calculated to be small for the in-plane deformations and are zero by symmetry for the out-of-plane ones.

Introduction

Recently our group has proposed a model capable of accurately calculating infrared fundamental intensities of gas phase molecules as well as interpreting the underlying electronic density rearrangements occurring for their normal vibrations in terms of completely classical contributions [1,2]. This model is based on the Quantum Theory of Atoms in Molecules [3,4] (QTAIM) and explains the intensities as a sum of charge, charge flux, dipole flux (CCFDF) and interaction contributions. It has been successfully applied to several groups of molecules for which complete infrared fundamental intensities have been measured including the X_2CY

* Corresponding author. Tel.: +55 19 3521 3106.
E-mail addresses: wagner.richter@iqm.unicamp.br (W.E. Richter), arnfilho@iqm.unicamp.br (A.F. Silva), andrew.pitoli@iqm.unicamp.br (A.C.L. Pitoli), vazquez@iqm.unicamp.br (P.A.M. Vazquez), bruns@iqm.unicamp.br (R.E. Bruns).

1386-1425/$ - see front matter © 2013 Elsevier B.V. All rights reserved.
http://dx.doi.org/10.1016/j.saa.2013.07.005

(X = F, Cl; Y = O, S) molecules [5]. Here we report results of an application of the QTAIM/CCFDF model to the infrared fundamental intensities of BF_3 and BCl_3. Their intensities have been measured many years ago [6,7] and have been interpreted based on simple bond moment models. Interest centers on investigating their CCFDF parameters and comparing them to those previously determined for the isoelectronic F_2CO and Cl_2CS molecules. One can expect these CCFDF parameters to reflect the differences in the intensities of the BX_3 and X_2CY molecules owing to the relative electron deficiencies of the boron atoms as compared to carbon as well as to the more highly polar bonds in boron trifluoride. There has been much discussion debating whether the BF bond in BF_3 should be classified as covalent or ionic [8–11]. In a highly ionic molecule, for which electron densities are concentrated about the individual atoms, one would expect to observe small charge fluxes for vibrational distortions compared with those found for covalent bonds. Furthermore the Quantum Theory Atoms In Molecules (QTAIM) approach evaluates parameters that can be used as an ionicity threshold, such as the Laplacian of the electronic density at the bond critical point [3]. One would expect to find consistency between the QTAIM/CCFDF parameters and the AIM parameters obtained from the electronic density distribution.

Calculations

The infrared intensity of the jth fundamental band is proportional to the square of the dipole moment derivative with respect to the normal coordinate [12], Q_j

$$A_j = \frac{N\pi}{3c^2}\left(\frac{\partial \vec{p}}{\partial Q_j}\right)^2. \quad (1)$$

The QTAIM charge–charge flux–dipole flux (CCFDF) model [1,2] partitions the Cartesian components, $\sigma = x, y$ or z, of the total dipole moment derivative into charge (C), charge flux (CF) and dipole flux (DF) contributions,

$$\frac{\partial p_\sigma}{\partial Q_j} = \left(\frac{\partial p_\sigma}{\partial Q_j}\right)_C + \left(\frac{\partial p_\sigma}{\partial Q_j}\right)_{CF} + \left(\frac{\partial p_\sigma}{\partial Q_j}\right)_{DF} \quad (2)$$

where

$$\left(\frac{\partial p_\sigma}{\partial Q_j}\right)_C = \sum_i q_i \partial \sigma_i / \partial Q_j$$

is the equilibrium atomic charge, q_i, $i = 1,2,\ldots,N$, contribution owing to movements of the N atoms along each of the Cartesian axes for the Q_jth normal coordinate,

$$\left(\frac{\partial p_\sigma}{\partial Q_j}\right)_{CF} = \sum_i \partial q_i / \partial Q_j \sigma_i$$

is the charge flux contribution, a sum of Cartesian weighted atomic charge derivatives with respect to the jth normal coordinate and

$$\left(\frac{\partial p_\sigma}{\partial Q_j}\right)_{DF} = \sum_i \partial m_{i,\sigma} / \partial Q_j$$

is the dipole flux contribution, a sum of the atomic dipole derivatives for each Cartesian component. Their contributions to the infrared intensity are

$$A_j = \left(\frac{N\pi}{3c^2}\right)\left[\left(\frac{\partial p_\sigma}{\partial Q_j}\right)_C^2 + \left(\frac{\partial p_\sigma}{\partial Q_j}\right)_{CF}^2 + \left(\frac{\partial p_\sigma}{\partial Q_j}\right)_{DF}^2 + 2\left(\frac{\partial p_\sigma}{\partial Q_j}\right)_C\left(\frac{\partial p_\sigma}{\partial Q_j}\right)_{CF} + 2\left(\frac{\partial p_\sigma}{\partial Q_j}\right)_C\left(\frac{\partial p_\sigma}{\partial Q_j}\right)_{DF} + 2\left(\frac{\partial p_\sigma}{\partial Q_j}\right)_{CF}\left(\frac{\partial p_\sigma}{\partial Q_j}\right)_{DF}\right] \quad (3)$$

The first three squared terms represent the charge, charge flux and dipole flux contributions to the jth fundamental vibrational intensity. The last three terms correspond to interactions between charge, charge flux and dipole flux contributions and can be positive when both derivative contributions are of the same sign reinforcing the total intensity or negative when the contributions have opposite signs decreasing the total intensity value. The intensity contributions in Eq. (3) can be expressed conveniently by

$$A_i = A_i^{(C)} + A_i^{(CF)} + A_i^{(DF)} + A_i^{(C\times CF)} + A_i^{(C\times DF)} + A_i^{(CF\times DF)}. \quad (4)$$

Electronic structure calculations were carried out on an AMD 64 Opteron workstation at the optimized theoretical geometries using the Gaussian03 [13] program as described previously [1,2]. The 4–31G, 6–31G, 6–31G(d,p), 6–31G(2d,2p), 6–31G(3d,3p), 6–31G+(2d,2p), 6–31G++(2d,2p), 6–31G+(3d,3p), 6–31G++(3d,3p), 6–311G, 6–311G(d,p), 6–311G(2d,2p), 6–31G(3d,3p), cc–pVDZ, cc–pVTZ and D95 basis sets were investigated at both the MP2 and the QCISD levels. Some of these basis sets were used in B3LYP and PBE1PBE DFT calculations. The MORPHY98 program [14] used the Gaussian03 output to calculate atomic charges and atomic dipoles at the optimized theoretical geometry and at distorted geometries with atoms displaced by 0.01 Å along the negative and positive directions of all three Cartesian coordinate axes. The PLACZEK program [15,16] was used to prepare all necessary input to run Gaussian03 single point calculations, to calculate the dipole moment derivatives and their CCFDF contributions with respect to atomic Cartesian coordinates, the atomic polar tensors, [17,18] and to transform these into derivatives with respect to normal coordinates. The boron atoms were placed at the origin of the Cartesian coordinate system with one bond along the positive x-axis and all atoms in the xy plane as in Fig. 1 of Ref. [20].

Results

The infrared intensities were calculated from wave functions obtained with the 16 different basis sets at the MP2 and QCISD levels. Furthermore several calculations using the B3LYP and PBE1PBE density functionals were carried out. These values are given as supplementary information in Table S1. The level of electron correlation treatment, MP2 or QCISD, made very little difference in the calculated intensity values. But these values were quite sensitive to the basis set chosen. Use of the 6–31G(2d,2p) set provided the most accurate results. The MP2, QCISD, B3LYP and PBE1PBE results with this basis resulted in root mean square errors of 11.3, 13.7, 24.0 and 20.7 km mol^{-1}, respectively, well within the 10% reported maximum experimental error in the intensity sum [6], 83.3 km mol^{-1}. The next closest results to the experimental values were obtained at both the MP2 and QCISD levels with the 6–311G(2d,2p) and 6–311G(3d,3p) basis sets with rms errors between 39.3 and 43.0 km mol^{-1}. Table 1 contains the results for the experimental intensities of BF_3 and BCl_3 along with those calculated with the 6–31G(2d,2p) basis set at the MP2, QCISD, B3LYP and PBE1PBE levels. The agreement between all these calculated results and the experimental BF_3 intensity values is very good.

The QTAIM/CCFDF parameters were calculated with all the basis sets at the MP2 level and are given in supplementary Table S2. Included also in this table are QCISD, B3LYP, and PBE1PBE levels results for the 6–31G(2d,2p) basis set. Inspection of the results there shows that all the CCFDF parameters for calculations using polarization functions in the basis set are quite similar whereas those from 4–31G, 6–31G, 6–311G and D95 basis sets are very different. This was confirmed by multivariate principal component analysis [19]. The averages and standard deviations of the parameters obtained from the basis sets with polarization functions are given in Table 2. As can be seen there all the CCFDF parameters with large averages indicating important contributions to the

Table 1
Experimental frequencies, intensities and calculated intensities (km mol^{-1}) for BF_3 and BCl_3, using the 6–31G(2d,2p) basis set.

Molecule	ν_{exp} (cm^{-1})			MP2	QCISD	B3LYP	PBE1PBE	Experimental[a]
BF_3	Q_2	720	A_2''	90.6	94.4	82.0	84.1	74.4
	Q_3	1505	E'	748.3	749.7	717.0	728.4	737.0
	Q_4	482		22.2	22.8	21.5	21.8	21.3
BCl_3	Q_2	455	A_2''	7.9	8.8	7.2	6.6	1.5
	Q_3	956	E'	765.6	734.6	713.0	720.9	231.3
	Q_4	249		2.0	2.0	1.5	1.5	0.8

[a] Experimental intensities from Refs. 6,7. The experimental error estimated by McKean for the BF_3 intensities is less than 10%; for BCl_3, errors were not reported.

fundamental intensities have relatively small standard deviations. Even though the theoretical intensity results vary with the basis set chosen the corresponding CCFDF parameter values are relatively insensitive to basis set changes as long as they contain polarization functions and their interpretations of the important electronic density changes occurring for the BF_3 vibrations are very similar.

The CCFDF contributions to the fundamental intensities calculated at the MP2/6–31G(2d,2p) level for BF_3 and related molecules are given in Table 3. The MP2/6–31G(2d,2p) values are very similar to the averages for BF_3 in Table 2 and are a logical choice for interpretation of the electronic changes occurring for its vibrations.

The theoretical values of the in-plane (A_4) and out-of-plane (A_2) bending intensities of BCl_3 are in reasonable agreement with the low experimental intensity values. However the theoretical stretching intensities (A_3) are about three times larger than the reported experimental intensity. For the basis sets studied here at the MP2, QCISD and DFT levels the rms errors vary between 229.7 and 371.2 km mol^{-1}. For all calculations the stretching intensity is always two to three times larger than the reported experimental value as can be seen in supplementary Table S1.

Since the intensity values are sensitive to basis set changes but not to the level of electron correlation treatment additional calculations were carried out with the aug–cc–pVNZ (N = D, T, Q, 5) basis sets at the MP2 level. The resulting A_3 values were 732.4, 727.4, 728.6 and 730.1 km mol^{-1}, respectively, in good agreement with those from the more modest basis sets. Furthermore calculations at the CCSD(T) correlation level with an aug–cc–pVTZ basis set also provides a similar value, 695.4 km mol^{-1} compared with a value of 703.9 km mol^{-1} for this basis set at the QCISD level. The CCSD(T) level combined with large basis sets has been shown to provide accurate intensity values for a large series of molecules [20,21]. It is difficult to conclude that all these theoretical A_3 values are so much in error considering the excellent agreement obtained for BF_3 above and the one reported for the isoelectronic Cl_2CS molecule with an rms error of only 13.0 km mol^{-1} when compared to its experimental fundamental intensity values [1].

Fortunately, new infrared gas phase spectra for both the BF_3 and BCl_3 molecules recently became available in a new database [22], provided by the Pacific Northwest National Laboratory (PNNL). Comparing the composite spectra of these two substances at equivalent molar concentration × pathlength values the relative areas of the stretching bands, yields a BF_3/BCl_3 ratio of 1.3. The theoretical intensity values for these bands are very similar for both molecules in agreement with this ratio. As such it is difficult accept a BCl_3 experimental intensity value that is three times smaller than the BF_3 value which is in excellent agreement with its theoretical estimates.

CCFDF parameters of BCl_3 were calculated for all the wave functions determined at the MP2 level as well as for the QCISD, B3LYP and PBE1PBE results for the 6–31G(2d,2p) basis set. These results are also given in supplementary Table S2. In order to investigate the sensitivities of these parameters to basis set changes a principal component analysis (PCA) of the QTAIM/CCFDF values for BCl_3 was carried out. PCA permits a two or three dimensional graphical examination of variations in higher order data. The QTAIM/CCFDF space has 18 dimensions since each of the three BCl_3 intensities are described by six CCFDF parameters (Eq. (4)). As such a 19 × 18 data matrix, where each row corresponds to a different quantum calculation and each column to a CCFDF parameter was subjected to PCA.

The principal component score graph is shown in Fig. 1. This graph is a two dimensional projection of 18 dimensional CCFDF space where the different quantum levels are represented by points in the graph. This graph describes 94.8% of the total data variance in the data set. As such two points that are close together on the two dimensional projection are probably in close proximity in the 18 dimensional space. The group of points on the right side of the PC graph have similar CCFDF values and correspond to basis sets with polarization functions at the MP2, QSISD and DFT levels.

Table 2 also contains the average and standard deviations of the intensity contributions for the three normal modes of BCl_3 of all the basis sets and electron correlation levels of the points on the right side of Fig. 1. These levels and basis sets are the same as those included in the average and standard deviation calculations for BF_3. The standard deviations are about one-third or less than their respective averages for all the important contributions of BCl_3. As such similar interpretations of the electronic density changes during the BCl_3 vibrations will be made so long as the basis set contains polarization functions.

The CCFDF contributions to the fundamental intensities calculated at the MP2/6–31G(2d,2p) level for BF_3, BCl_3, F_2CO and Cl_2CS are given in Table 3. Note that the CCFDF values for the MP2/6–31G(2d,2p) wave function are very close to the average values in Table 2. This is consistent with the principal component graph for BCl_3 in Fig. 1 where the point corresponding to the MP2/6–31G(2d,2p) result is near the center of the group of points for

Table 2
Averages and standard deviations of QTAIM/CCFDF parameter values for selected[a] basis set results (km mol^{-1}).

	Q_2		Q_{3a}		Q_{4a}	
BF_3						
$A^{(C)}$	651.2	±17.3	585.1	±15.7	66.1	±2.3
$A^{(CF)}$	0.0		3.9	±2.3	0.2	±0.1
$A^{(DF)}$	241.4	±13.2	3.3	±2.0	24.5	±0.9
$A^{(C\times CF)}$	0.0		−93.0	±23.6	6.3	±1.9
$A^{(C\times DF)}$	−792.8	±31.4	−82.2	±33.2	−80.5	±2.0
$A^{(CF\times DF)}$	0.0		6.2	±3.0	−3.8	±1.2
BCl_3						
$A^{(C)}$	410.8	±14.8	384.9	±13.9	25.9	±1.1
$A^{(CF)}$	0.0		79.1	±25.8	0.8	±0.3
$A^{(DF)}$	317.0	±20.0	81.2	±32.5	25.8	±1.0
$A^{(C\times CF)}$	0.0		−344.5	±54.0	9.0	±1.3
$A^{(C\times DF)}$	−721.6	±34.6	346.3	±67.4	−51.7	±1.8
$A^{(CF\times DF)}$	0.0		−159.7	±57.5	−9.1	±1.4

[a] 6–31G(3d,3p), 6–31G+(2d,2p), 6–31G++(2d,2p), 6–31G+(3d,3p), 6–31G++(3d,3p), 6–311G(d,p), 6–311G(2d,2p), 6–311G(3d,3p), cc–pVDZ and cc–pVTZ at the MP2 level, plus 6–31G(2d,2p) at MP2, QCISD, B3LYP and PBE1PBE levels.

Table 3
CCFDF contributions for normal modes of the investigated molecules calculated at the MP2/6–31G(2d,2p) level for the polyatomic molecules and QCISD/6–311++G(d,p) for the diatomic ones (km mol^{-1}).

Molecule	Mode	C^2	CF^2	DF^2	$2(C \times CF)$	$2(C \times DF)$	$2(CF \times DF)$	Total
BF_3	Q_2	651.8	0.0	257.4	0.0	−819.1	0.0	90.1
	Q_{3a}	588.1	5.6	6.2	−115.0	−121.1	11.8	375.6
	Q_{4a}	64.3	0.1	25.9	5.5	−81.6	−3.5	10.7
F_2CO	Q_1	537.5	751.6	541.4	−1271.2	1078.9	−1275.8	362.4
	Q_2	19.5	9.2	33.8	−26.8	51.3	−35.2	51.8
	Q_3	28.4	4.1	25.4	21.7	−53.7	−20.5	5.4
	Q_4	492.5	201.0	125.5	−629.2	497.2	−317.6	369.4
	Q_5	90.9	11.0	106.0	63.1	−196.3	−68.1	6.6
	Q_6	581.6	0.0	342.8	0.0	−893.0	0.0	31.4
Cl_2CS	Q_1	8.1	2277.2	876.9	−272.1	168.8	−2826.2	232.7
	Q_2	1.9	0.8	18.2	−2.5	11.8	−7.8	22.4
	Q_3	0.8	0.0	0.1	−0.3	−0.5	0.1	0.2
	Q_4	3.2	210.6	4.9	−51.7	−7.9	64.1	223.2
	Q_5	4.9	0.1	2.0	−1.7	−6.2	1.1	0.2
	Q_6	5.2	0.0	1.1	0.0	−4.8	0.0	1.5
BCl_3	Q_2	400.2	0.0	295.7	0.0	−688.1	0.0	7.8
	Q_{3a}	374.4	98.5	101.6	−394.0	390.1	−200.1	370.5
	Q_{4a}	25.2	0.8	24.6	9.1	−49.9	−9.0	0.8
CF_4	Q_{3a}	660.8	88.5	14.9	−483.7	198.69	−72.7	406.5
Diatomics								
LiCl		141.9	3.3	4.4	43.4	−49.7	−7.6	135.7
LiF		164.0	2.7	3.6	42.2	−48.7	−6.3	157.5
NaCl		57.0	1.5	1.7	18.7	−19.8	−3.2	55.9
NaF		78.7	6.1	3.9	43.9	−35.0	−9.8	87.8
LiH		906.6	4.3	198.6	−125.1	−848.7	58.6	194.3
HF		505.1	168.1	2.6	−582.9	72.2	−41.6	123.5
HCl		54.3	101.2	163.4	148.3	−188.4	−257.1	21.7
HBr		1.6	462.3	450.2	−53.5	52.8	−912.5	0.9
CO		191.2	247.6	111.9	−435.2	292.6	−332.9	75.2

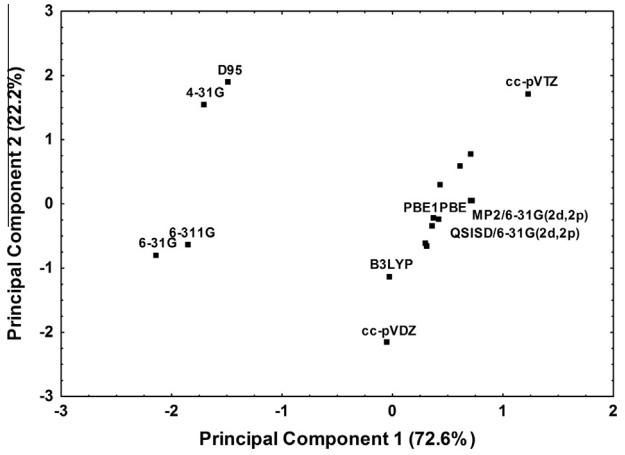

Fig. 1. Principal component graph of the QTAIM/CCFDF parameters of BCl_3 for the sixteen basis sets investigated at the MP2 electron correlation treatment level and for the QCISD, B3LYP and PBE1PBE calculations with the 6–31G(2d,2p) basis set.

Table 4
Experimental[a] and MP2/6–31G(2d,2p) calculated atomic polar tensors for BF_3 and BCl_3 (Units of electrons, e).

BF_3		dPx	dPy	dPz	BCl_3		dPx	dPy	dPz
Experimental									
B	dx	1.86	0	0	B	dx	1.06	0	0
	dy	0	1.86	0		dy	0	1.06	0
	dz	0	0	0.83		dz	0	0	0.12
F	dx	−0.82	0	0	Cl	dx	−0.55	0	0
	dy	0	−0.42	0		dy	0	−0.15	0
	dz	0	0	−0.28		dz	0	0	−0.04
Calculated									
B	dx	1.88	0	0	B	dx	1.94	0	0
	dy	0	1.88	0		dy	0	1.94	0
	dz	0	0	0.92		dz	0	0	0.28
F	dx	−0.86	0	0	Cl	dx	−1.08	0	0
	dy	0	−0.39	0		dy	0	−0.21	0
	dz	0	0	−0.30		dz	0	0	−0.09

[a] Ref. [20].

CCFDF values obtained using polarization functions in the basis set. As such the MP2/6–31G(2d,2p) wave function parameters are taken to interpret the electronic changes for the BCl_3 vibrations.

Table 4 contains the experimental [23] and calculated at MP2/6–31G(2d,2p) results for the atomic polar tensors of the boron, fluorine and chlorine atoms of BF_3 and BCl_3. The calculated polar tensor elements for BF_3 are in excellent agreement with the experimental values, the differences being well within 0.1 e. However some of the calculated BCl_3 polar tensor elements are about twice as large in absolute magnitude as the tensor elements calculated from the experimental intensities. This of course was anticipated since the largest BCl_3 calculated intensity, A_{3a}, is almost four times larger than the reported experimental value and dwarfs the other two fundamental intensity values. The corresponding CCFDF contributions for the mean dipole moment derivatives of these molecules, one-third the trace of the atomic polar tensor, are given in Table 5.

The QTAIM charge on boron of 2.49 e (Table 5) in BF_3 can be compared with the GAPT charge [24] (one-third of the trace of the boron polar tensor in Table 4) of 1.56 e and an IR charge [25–27] of 0.83 (dp_z/dz_B also in Table 4). The GAPT and IR charges are obtained only from experimental data. The GAPT charge contains dynamic contributions from charge flux and dipole flux whereas the QTAIM charge does not. The IR charge is about one-third of the value of the QTAIM charge. However IR charges

Table 5
CCFDF contributions for the mean dipole derivative of BF_3, BCl_3, F_2CO and Cl_2CS (in electrons, *e*).

Molecule	Atom	Charge	Charge flux	Dipole flux	*C* + *CF* + *DF*
BF_3	B	2.487	−0.140	−0.779	1.567
	F	−0.829	0.046	0.260	−0.522
F_2CO	C	2.391	−1.255	0.355	1.492
	O	−1.165	0.609	0.010	−0.546
	F	−0.613	0.323	−0.183	−0.473
BCl_3	B	2.025	−0.632	−0.004	1.388
	Cl	−0.675	0.210	0.001	−0.462
Cl_2CS	C	−0.228	2.067	−0.834	1.005
	S	0.445	−1.371	0.659	−0.267
	Cl	−0.108	−0.348	0.087	−0.369

are obtained assuming the existence of only atomic charges whereas QTAIM uses both atomic charges and atomic dipoles to describe the molecular electrostatic potential. CHELPG charges [28,29] for BF_3 calculated at the MP2/6–31G(2d,2p) level are $q_B = 0.90$ *e* and $q_F = -0.30$ *e*. These charges are very similar to the experimental IR charges but much different from the QTAIM values. Terrabuio and Haiduke [30] have shown that even though QTAIM and CHELPG charges can have very different values the molecular electrostatic potential owing to CHELPG charges at large distances from the molecule are very similar to the potentials calculated using QTAIM atomic charges and atomic dipoles. The QTAIM charges are also larger than the GAPT, IR and CHELPG (at MP2/6–31G(2d,2p) level) for BCl_3.

Discussion

The BF_3 and BCl_3 stretching vibrational modes (ν_{3a}) have very similar total intensity values at the MP2/6–31G(2d,2p) level, 375.6 and 370.5 km mol^{-1}, respectively, that are predominantly determined by equilibrium charge movements as can be seen in Table 3. The charge separations in BF_3, $q_B = +2.49$ *e* and $q_F = -0.83$ *e*, are larger than those in BCl_3, $q_B = +2.03$ *e* and $q_{Cl} = -0.68$ *e* (see Table 5). However the charge–charge flux and charge–dipole flux interactions are both negative in BF_3 indicating that both fluxes have dipole derivative contributions that are opposite in direction to the one owing to the movements of equilibrium charge. This results in the partial cancelation of derivative contributions diminishing the total intensity. The corresponding dipole moment derivative contributions are diagrammed on the upper left of Fig. 2. The BF_3 molecule has small charge and dipole flux contributions to the total dipole moment derivative, −0.076 and −0.080 eu^{½}, respectively, compared with an equilibrium charge contribution of +0.777 eu^{½}. However owing to the squared relation between the dipole moment derivative and intensity these small dipole derivative contributions are very effective in substantially reducing the fundamental intensity by means of their interactions with the large equilibrium charge contribution.

In contrast the BCl_3 stretching intensity has a smaller equilibrium charge contribution than does BF_3. In fact this contribution of 374.4 km mol^{-1} is almost the same as the total calculated intensity, 380.5 km mol^{-1}. This occurs owing to an almost perfect cancelation of charge and dipole flux contributions, $A_{C\times CF} + A_{C\times DF} = -3.9$ km mol^{-1} and $A_{CF} + A_{DF} + A_{CF\times DF} = 0.0$ km mol^{-1}. As such only the equilibrium charge movements are necessary to explain the intensity of the υ_3 band of BCl_3. The schematic diagram in Fig. 2 for Q_{3a} of BCl_3 contains its CCFDF dipole moment derivative polarities and values. The charge flux dipole moment derivative is of opposite sign and almost equal value to the dipole flux one.

A comparison of the isoelectronic BF_3 and F_2CO stretching intensity contributions given in Table 3 is of interest since BF_3 is

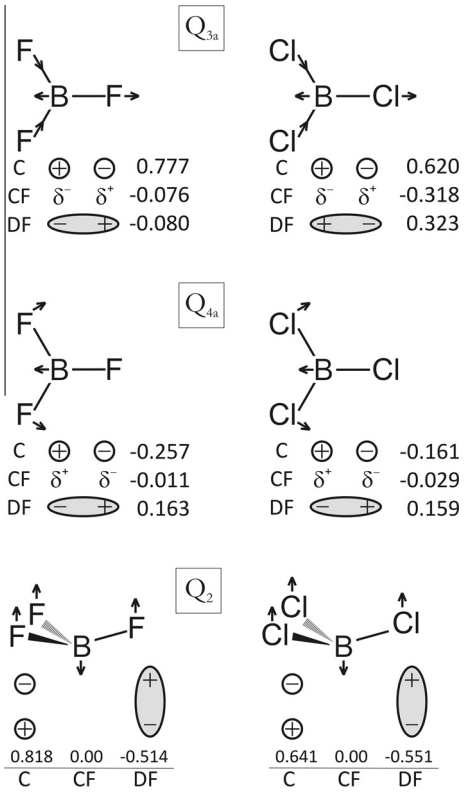

Fig. 2. Schematic diagrams of electronic distortions of the BF_3 and BCl_3 normal vibrations. Charge (*C*), charge flux (*CF*) and dipole flux (*DF*) contribution values are given along with the direction of the polarity changes.

an electron deficient molecule whereas F_2CO is not. In spite of this the doubly degenerate υ_3 stretching fundamentals have a calculated intensity of 751.2 km mol^{-1} compared with a sum of the C═O and C—F stretching intensities that is almost the same, 731.8 km mol^{-1}. The corresponding experimental values [31] are 737.0 and 752.5 km mol^{-1}. The equilibrium charge contributions are similar in both molecules, 588.1 km mol^{-1} for BF_3 compared with the F_2CO average value of 515.0 km mol^{-1}, but the charge and dipole fluxes are very large in F_2CO (averages of 476.3 and 333.5 km mol^{-1}) compared to those for BF_3 (5.6 and 6.2 km mol^{-1}). These contributions cancel one another for F_2CO, the $A_{CF} + A_{DF} + A_{CF\times DF}$ sums are only 8.9 km mol^{-1} for Q_1 and 17.2 km mol^{-1} for Q_4. So the stretching intensity sums are very similar for F_2CO and BF_3 although electronic density rearrangements on bond stretching are very different with small fluxes for BF_3 and large canceling ones for F_2CO.

The QTAIM/CCFDF contributions to the dipole moment derivative of the BF_3 stretching mode consisting of a large equilibrium charge contribution and dynamic contributions that are much

smaller are consistent with results found for highly ionic molecules. Included in Table 3 are QTAIM/CCFDF contributions calculated at the 6–311++G(d,p) level for a group of diatomic molecules for which experimental infrared intensities or dipole moment derivatives have been measured. Calculations at this level resulted in accurate estimates of their mean dipole moment derivatives, within 0.025 *e*. As can be seen in Table 3 the highly ionic diatomic molecules, LiF, LiCl, NaCl, and NaF are characterized by large equilibrium charge contributions, between 57 and 164 km mol^{-1}, and very small charge flux and dipole flux contributions, less than 6.1 km mol^{-1} at the QCISD/6–311++G(d,p) level. This pattern is similar to the one observed for the BF_3 stretching vibration for which the equilibrium charge contribution of 588.1 km mol^{-1} is about a hundred times larger than the flux contributions of 5.6 and 6.2 km mol^{-1}. On the other hand the CF_4 molecule with large charge and charge flux contributions of 660.8 and 88.5 km mol^{-1}, respectively, is not considered to be ionic, although it has very polar bonds. The charge flux contributions are also large in the covalent HF, HCl, HBr and CO molecules ranging from 101.2 to 247.6 km mol^{-1}.

QTAIM analysis of the equilibrium electron charge density also provides evidence of the ionicity of the BF_3 bonds. The Laplacian of the electronic density at the bond critical points in BF_3 is +1.23 indicating depletions of electron densities in the bonding regions relative to the high densities concentrated around the nuclei. This compares with positive values in the 0.20 and 0.66 range of the Laplacian at the bond critical points of NaF, NaCl, LiF and LiCl. In contrast these Laplacian values are negative, between −0.50 and −3.15 for HF, HCl, HBr and CF_4.

The doubly degenerate stretching intensity calculated for BCl_3 of 741.0 km mol^{-1} is much larger than the sum of the C═S and C—Cl stretching intensities in Cl_2CS, 455.7 km mol^{-1}. Whereas the BCl_3 stretches are characterized by large equilibrium charge contributions, as discussed above, the C═S and C—Cl stretches have much larger flux contributions but very small equilibrium charge ones, 8.1 and 3.2 km mol^{-1}. These large flux contributions only partially cancel for Cl_2CS resulting in total MP2/6–31G(2d,2p) intensity values of 232.7 km mol^{-1} for the C═S stretch and 223.2 km mol^{-1} for the C—Cl stretch. These values can be compared with the experimental values [32] of 210.8 and 162.9 km mol^{-1}.

Even though the equilibrium charge contribution, 374.4 km mol^{-1}, is dominant for the BCl_3 stretching vibration its flux parameters are not negligible having values close to 100 km mol^{-1}. Covalent molecules with polar bonds like CF_4 and HF have large charge flux contributions of 88.5 and 168.1 km mol^{-1}, respectively, (see Table 3). As stated above less polar covalent molecules like HCl, HBr and CO have flux contributions that are all larger than 100 km mol^{-1}. This indicates that the ionicity of the BCl_3 bonds is much less than those of BF_3 as might have been anticipated.

The ν_{4a} in-plane deformations of both BF_3 and BCl_3 have very small intensities and can be accurately described by only equilibrium charge movement and atomic dipole fluxes. Fig. 2 contains diagrams representing the electronic density distortion along with the values of the dipole moment derivative contributions for BF_3 and BCl_3. The charge flux dipole derivative contributions for both molecules are about an order of magnitude smaller than the equilibrium charge and dipole flux contributions. As such all contributions involving the charge flux for the ν_{4a} intensities of BF_3 and BCl_3 in Table 3 are seen to be negligible. The BF_3 contributions from the charge, dipole flux and their interaction sum to 8.6 km mol^{-1} close to its total calculated intensity of 10.7 km mol^{-1}. In BCl_3 these contributions sum to −0.1 km mol^{-1} close to the small calculated intensity of 0.9 km mol^{-1}, which is in very good agreement with the experimental value of 0.8 km mol^{-1}.

The electronic density rearrangements for the out-of-plane vibrations of BF_3 and BCl_3 are very similar as can be seen in Fig. 2 although the experimental intensity for BF_3 of 74.4 km mol^{-1} is appreciably larger than the one for BCl_3, 1.5 km mol^{-1}. Out-of-plane intensities, of course, have zero charge flux contributions by symmetry. As such only the equilibrium charge and dipole flux and their interaction contribute to the total intensity. The dipole moment changes owing to equilibrium charge movements are partially canceled by the dipole flux ones for both molecules. The equilibrium charge, dipole flux and charge–dipole flux interaction terms sum to 90.0 and 7.9 km mol^{-1} reproducing the calculated total intensities which are comparable to the experimental values given above.

The out-of-plane deformations in BF_3 and F_2CO have large equilibrium charge and dipole flux intensity contributions that are mostly canceled by their charge–dipole flux interactions, i.e. the equilibrium charge and dipole flux contributions to the dipole moment derivative are in opposite directions. As such the out-of-plane bands of both molecules are only moderately intense.

The ν_2 BCl_3 and ν_6 Cl_2CS out-of-plane intensities are both very small although the electronic density rearrangements for their out-of-plane vibrations are very different. All the intensity contributions for Cl_2CS are very small contrary to the large canceling contributions for BCl_3.

Table 5 contains the mean dipole moment derivatives as well as their charge, charge flux and dipole flux contributions. The charge contributions to the dipole moment derivative are identical to the zero flux charges as calculated by QTAIM. The zero flux charge on boron, 2.49 *e*, in BF_3 is only about 0.1 *e* more positive than the one on carbon in F_2CO, 2.39 *e*. As a consequence the sum of negative charges on the terminal atoms is very similar for both molecules. The charge flux contributions of all the F_2CO atoms are substantially larger than those of the BF_3 atoms. In contrast the dipole flux contributions to the mean derivatives of BF_3 are somewhat larger than those for F_2CO.

No similarities are found for the dipole moment derivative values of BCl_3 and Cl_2CS. The zero flux charges are very different. Even the charge on carbon (−0.23 *e*) is of opposite sign to the one on boron (+2.03 *e*). Sulfur has a positive charge (+0.45 *e*) and the Cl_2CS chlorine atoms have a relatively small negative charge (−0.11 *e*) compared to those in BCl_3 (−0.68 *e*) The charge and dipole flux contributions to the mean derivatives of all the Cl_2CS atoms have absolute values much greater than those for BCl_3.

Conclusion

In summary, the QTAIM/CCFDF model interprets the dipole moment changes occurring for the BF_3 and BCl_3 stretching vibrations by predominant equilibrium atomic charge movements. In BF_3 small dynamic flux contributions of opposite sign partially cancel the equilibrium charge contribution but in BCl_3 the dynamic contributions almost exactly cancel one another permitting its stretching intensity to be accurately described by movements of the q_B = +2.03 *e* and q_{Cl} = −0.68 *e* equilibrium zero flux atomic charges. In our previous study [1] the CF stretching intensities of the difluoroethylenes, X_2CY molecules and the fluorochloromethanes were accurately estimated by summing the charge, charge–charge flux and charge–dipole flux contributions. For the doubly degenerate stretching intensity of BF_3 this sum results in 704 km mol^{-1} compared with the experimental value of 737 km mol^{-1}. The BF_3 stretching vibration provokes a very small charge flux providing evidence of the ionic character of the BF_3 bonds. This is consistent with positive values of the Laplacian of the electronic density determined at the bond critical points.

For the BCl_3 stretching intensity the charge, charge–charge flux and charge–dipole flux sum, 741 km mol^{-1}, happens to be in exact agreement with the calculated MP2/6–311G(2d,2p) value since the

charge flux and dipole flux contributions are exactly canceled by the charge flux–dipole flux interaction. This sum normally does not provide accurate estimates for the CCl stretching intensities since the charge contribution is not the dominant one.

The QTAIM/CCFDF interpretation of both the in-plane and out-of-plane bending intensities of these molecules consists of equilibrium charge movements with compensating atomic electron density polarizations in the opposite direction. This also appears to be characteristic of most CF and CCl bends. Fifteen of the 18 CF bends for the dihaloethylenes, X_2CY molecules and the fluorochloromethanes have predominant positive charge and dipole flux contributions that are partially compensated by negative charge–dipole flux interaction contributions. Furthermore this behavior is found for 9 of the 11 CCl bends in these molecules. When compared with bond moment model interpretations the important difference is the polarizations of atomic electron densities which are included as atomic dipole flux intensity contributions in the QTAIM/CCFDF model. On the other hand the QTAIM/CCFDF model results indicate small charge flux contributions to the deformation intensities as is assumed in the bond moment model.

Acknowledgements

We thank the teams at PNNL and NIST for the construction, maintenance and free accessibility of their databases [33]. W.E.R., A.F.S. and A.C.L.P. thank CNPq (Conselho Nacional de Desenvolvimento Científico e Tecnológico) for graduate student fellowships and R.E.B. thanks CNPq for a research fellowship. We are grateful to FAPESP (Fundação de Amparo à Pesquisa do Estado de São Paulo) for partial financial support of this work.

Appendix A. Supplementary material

Supplementary data associated with this article can be found, in the online version, at http://dx.doi.org/10.1016/j.saa.2013.07.005.

References

[1] A.F. Silva, W.E. Richter, H.G.C. Meneses, S.H.D.M. Faria, R.E. Bruns, J. Phys. Chem. A 116 (2012) 8238–8249.
[2] R.L.A. Haiduke, R.E. Bruns, J. Phys. Chem. A 109 (2005) 2680.
[3] R.F.W. Bader, Atoms in Molecules: A Quantum Theory, Clarendon Press, Oxford, 1990.
[4] R.F.W. Bader, A. Larouche, C. Gatti, M.T. Carrol, P.J. MacDougall, K.B. Wiberg, J. Chem. Phys. 87 (1987) 1142.
[5] S.H.D.M. Faria, J.V. Silva Jr., R.L.A. Haiduke, L.N. Vidal, P.A.M. Vazquez, R.E. Bruns, J. Phys. Chem. A 111 (2007) 7870–7875.
[6] D.C. McKean, J. Chem. Phys. 24 (5) (1956) 1002.
[7] O. Brieux de Mandirola, Spectrochim. Acta A 23 (1967) 767.
[8] R.J. Gillespie, J. Chem. Educ. 75 (1998) 923.
[9] A. Haaland, T. Helgaker, K. Ruudand, D.J. Shorokhov, J. Chem. Educ. 77 (2000) 1076.
[10] E.A. Robinson, S.A. Johnson, T.H. Tang, R.J. Gillespie, Inorg. Chem. 36 (14) (1997) 3022.
[11] R.J. Gillespie, J. Chem. Educ. 78 (2001) 1688–1691.
[12] J. Overend, in: M. Davies (Ed.), Infrared Spectroscopy and Molecular Structure, Elsevier, New York, 1955.
[13] M.J. Frisch, G.W. Trucks, H.B. Schlegel, G.E. Scuseria, M.A. Robb, J.R. Cheeseman, J.A. Montgomery Jr., T. Vreven, K.N. Kudin, J.C. Burant, J.M. Millam, S.S. Iyengar, J. Tomasi, V. Barone, B. Mennucci, M. Cossi, G. Scalmani, N. Rega, G.A. Petersson, H. Nakatsuji, M. Hada, M. Ehara, K. Toyota, R. Fukuda, J. Hasegawa, M. Ishida, T. Nakajima, Y. Honda, O. Kitao, H. Nakai, M. Klene, X. Li, J.E. Knox, H.P. Hratchian, J.B. Cross, V. Bakken, C. Adamo, J. Jaramillo, R. Gomperts, R.E. Stratmann, O. Yazyev, A.J. Austin, R. Cammi, C. Pomelli, J.W. Ochterski, P.Y. Ayala, K. Morokuma, G.A. Voth, P. Salvador, J.J. Dannenberg, V.G. Zakrzewski, S. Dapprich, A.D. Daniels, M.C. Strain, O. Farkas, D.K. Malick, A.D. Rabuck, K. Raghavachari, J.B. Foresman, J.V. Ortiz, Q. Cui, A.G. Baboul, S. Clifford, J. Cioslowski, B.B. Stefanov, G. Liu, A. Liashenko, P. Piskorz, I. Komaromi, R.L. Martin, D.J. Fox, T. Keith, M.A. Al-Laham, C.Y. Peng, A. Nanayakkara, M. Challacombe, P.M.W. Gill, B. Johnson, W. Chen, M.W. Wong, C. Gonzalez, J.A. Pople, GAUSSIAN03 Revision D02, Gaussian, Inc., Wallingford, CT, 2004.
[14] MORPHY98, A program written by P.L.A. Popelier with a contribution from R.G.A. Bone, Manchester, England, EU, 1998.
[15] L.N. Vidal, P.A.M. Vazquez, Quim. Nova 26 (2003) 507.
[16] L.N. Vidal, P.A.M. Vazquez, Int. J. Quantum Chem. 103 (5) (2005) 632.
[17] J.F. Biarge, J. Herranz, J. Morcillo, Ann. R. Soc. Esp. Fis. Quim. A 57 (1961) 81.
[18] W.B. Person, J.H. Newton, J. Chem. Phys. 61 (1974) 1040.
[19] A.L.M.S. Azevedo, B. Barros Neto, I.S. Scarminio, R.E. Bruns, J. Comp. Chem. 17 (1996) 167–177.
[20] B. Galobov, Y. Yamaguchi, R.B. Remington, H.F. Schaefer III, J. Phys. Chem. A 106 (2002) 819.
[21] J.V. da Silva, L.N. Vidal, P.M.A. Vazquez, R.E. Bruns, Int. J. Quantum Chem. 110 (2010) 2029.
[22] S.W. Sharpe, T.J. Johnson, R.L. Sams, P.M. Chu, G.C. Rhoderick, P.A. Johnson, Appl. Spectrosc. 58 (2004) 1452.
[23] A.B.M.S. Bassi, R.E. Bruns, J. Chem. Phys. 64 (1976) 3053.
[24] J. Cioslowski, J. Am. Chem. Soc. 111 (1989) 8333.
[25] A. Milani, C. Castiglioni, J. Phys. Chem. A 114 (2010) 624.
[26] A. Milani, G. Galimberti, C. Castiglioni, G. Zerbi, J. Mol. Struct. 976 (2010) 342.
[27] A. Milani, C. Castiglioni, J. Mol. Struct. 955 (2010) 158.
[28] L.E. Chirlian, M.M. Franci, J. Comp. Chem. 8 (1990) 894.
[29] C.M. Breneman, K.B. Wiberg, J. Comp. Chem. 11 (1990) 361.
[30] L.A. Terrabuio, R.L.A. Haiduke, Int. J. Quantum Chem. 112 (2012) 3198.
[31] M.J. Hopper, J.W. Russell, J. Overend, J. Chem. Phys. 48 (1967) 3765.
[32] M.J. Hopper, J.W. Russell, J. Overend, Spectrochim. Acta A 28 (1972) 1215.
[33] <https://secure2.pnl.gov/nsd/nsd.nsf/Welcome>.